Mathematical Modeling of Hydromagnetic Squeeze Film in Longitudinally Rough Conducting Truncated Conical Plates Considering Slip Velocity

J. V. Adeshara[1], M. B. Prajapati[2], G. M. Deheri[3] and R. M. Patel[4]

1. Research Scholar, Department of Mathematics, H. N. G. University, Patan – 384 265, Gujarat State, India
2. Head, Department of Mathematics, H. N. G. University, Patan – 384 265, Gujarat State, India.
3. Department of Mathematics, S. P. University, Vallabh Vidyanagar – 388 120, Gujarat State, India.
4. Department of Mathematics, Gujarat Arts and Science College, Ahmedabad - 380 006 Gujarat State, India

***ABSTRACT*:**

An attempt has been made to discuss the behavior of a hydromagnetic fluid-based squeeze film between rough truncated conical plates by taking into consideration the effects of slip velocity. Beavers and Joseph's model has been adopted to incorporate the effect of slip velocity. Taking recourse to a different type of probability density function, the model of Christensen and Tonder has been adopted to evaluate the effect of longitudinal surface roughness and the concern stochastically averaged Reynolds' type equation has been solved to derive the expression for pressure distribution. This results in the calculation of load carrying capacity. The graphical representations make it clear that although the effect of slip velocity is relatively adverse the magnetic fluid lubricant saves the situation to a limited extent, at least in the case of the negatively skewed roughness. For an overall improvement of performance of bearing system, the slip parameter should be minimized. A suitable combination of aspect ratio and semi vertical anglemay lead to some compensation for negative effect of slip velocity, especially when variance (negative) is involved.

IndexTerms: Truncated conical plates, slip velocity, longitudinal roughness, conductivity, load bearing capacity.

NOMENCLATURE:

x, y	Cartesian coordinates
H	Lubricant film thickness
$\dot{h}$	Squeeze film velocity
μ	Viscosity
B_0	Uniform transverse magnetic field applied between the plates.
S	Electrical conductivity of the lubricant
M	$= B_0 h\left(\frac{s}{\mu}\right)^{1/2}$ = Hartmann number
d_0	Surface width of the lower plate
d_1	Surface width of the upper plate
s_0	Electrical conductivity of lower surface
s_1	Electrical conductivity of upper surface
S*	Non-dimensional slip parameter
$\phi_0(h)$	$= \frac{s_0 d_0}{sh}$ = Electrical permeability of the lower surface
$\phi_1(h)$	$= \frac{s_1 d_1}{sh}$ = Electrical permeability of the upper surface
ω	Semi vertical angle of the cone
p	Lubricant pressure
w	Load carrying capacity
σ^*	Non-dimensional standard deviation (σ/h)
α^*	Non-dimensional variance (α/h)
ε^*	Non-dimensional skewness (ε/h^3)
P	Non-dimensional pressure
W	Dimensionless load carrying capacity

I. INTRODUCTION:

Prakash and Vij [1] analyzed the squeeze films between porous plates of various shapes such as circular annular, elliptic, rectangular and conical. In this investigation a comparison was made between the squeeze film performances of various geometries of equivalent surface area with other parameters remaining the same and it was concluded that the circular plates had the highest transient load carrying capacity. The use of magnetic fluid as a lubricant modifying the performance of a bearing system has been explored and employed in a number of investigations [Verma [2]; Bhat and Deheri [3-4]]. This investigation established that the load carrying capacity increased with increasing magnetization. The squeeze film performance in circular disks had significantly improved as compared to that of the annular plates. Hsiu at el [5] studied the combined effect of couple stresses and roughness.

The transverse roughness caused the reduction in the attitude angle and friction parameters while the effect of longitudinal roughness remained almost opposite to that of transverse roughness. Deheri et al [6] extended the analysis of Bhat and Deheri [4] to study the effect of surface roughness on the performance of a magnetic fluid-based squeeze film between rough porous truncated conical plates. In this investigation Christensen and Tonder [7-9] stochastic model was adopted to evaluate the effect of transverse surface roughness. This investigation of Deheri et al [6] suggested that there was some scope for minimizing the adverse effect of roughness by the magnetization at least in the case of negative skewed roughness.

Gupta and Deheri [10] analyzed the effect of transverse surface roughness on the performance of a squeeze film in spherical bearing. It was found that among the three roughness parameters the skewness affected the system most and positively skewed roughness caused savoir load reduction. Andharia et al [11] discussed the effect of transverse surface roughness on the performance of a hydrodynamic slider bearing adopting the stochastic model and found that a transverse roughness resulted in an adverse effect in general. However, the situation remained comparatively better when variance (negative) was involved and this positive effect was aided by the negative skewed roughness. Hsu et. al. [12] investigated the combined effect of surface roughness and rotating inertia on the squeeze film performance characteristics of parallel circular disks. It was shown that the surface roughness turned in an adverse effect in general.

The rotating inertia further aggravated the situation when relatively higher values of standard deviation were involved. Schwarz [13] presented a new method to calculate the elastic deformation of a sphere on a flat surface considering the influence of short range and long-range attraction forces inside and outside the actual contact area. Shimpi and Deheri [14-15] extended and developed the analysis of Bhat and Deheri [3-4] respectively by considering the effect of surface roughness and deformation on the behaviour of a magnetic fluid based squeeze film in rotating curved porous circular plates. Here it was established that the deformation effect needed to be minimized to compensate the adverse effect of the porosity and standard deviation by the positive effect of magnetization. The negatively skewed roughness registered relatively more compensation. Shimpi and Deheri [16] made an effort to study the surface roughness effect on the squeeze film performance between a fluid circular plate under the presence of magnetic fluid. It was noticed that the positive effect of magnetization got a further boost in the presence of negatively skewed roughness.

Shah and Patel [17] discussed the slider bearing of various geometrical shapes incorporating the effects of anisotropic permeability and slip velocity. Mirea and Voicu [18] studied the load bearing capacity of the truncated cone and hemispherical foundations realized in punched holes by resorting to Finite Element Method. The results emphasized a better behaviour for the hemispherical element as compared to the truncated conical element. Ahmed and Mahdy [19] embarked on a non-similarity analysis for investigating the laminar free convection boundary layer flow over a permeable isothermal truncated cone in the presence of a transverse magnetic field effect. Further, various models of nano-fluid based on different formulae for thermal conductivity and dynamic viscosity on the flow and heat transfer characteristic were discussed. Nassab et al [20] numerically analyzed lubricant compressibility effect on hydrodynamic characteristics of heavily loaded journal bearings. The result showed that the compressibility effect caused an increase in the generated hydrodynamic pressure. Rahmatabadi and Rashidi [21] presented the study of the effect of the mount angle on the theoretical static and dynamic characteristics of three types of gas lubricated non circular journal bearings. It was found that the effect of mount angel was more significant at low compressibility number. Nassab and Moayeri [22] dealt with the two-dimensional thermo-hydrodynamic analysis of journal bearing characteristics.

Shimpi and Deheri [28] considered the effect of slip velocity on ferrofluid based truncated conical plates. Therefore, it was sought to study the effect of velocity slip on hydromagnetic squeeze film between conducting transversely rough truncated conical plates.

II. ANALYSIS:

The bearing system consists of two truncated conical plates. The upper plate moves towards the lower plate. The bearing surfaces are longitudinally rough and the backed by solid facing. The geometry and coordinates are depicted in the following Figure.

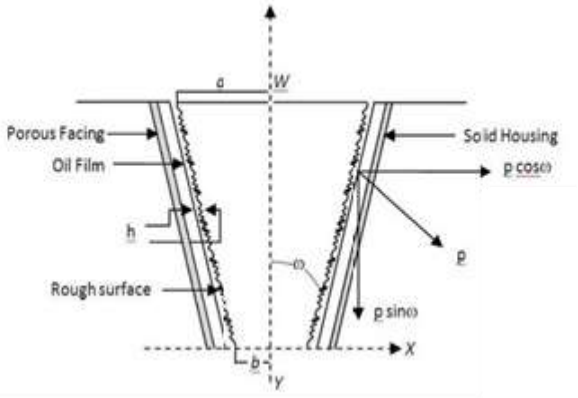

Fig. 1. Configuration of truncated conical plates

The plates are considered to be electrically conductive and a lubricant that conducts electrically fills the clearance space between them. Between the plates is applied a uniform transverse magnetic field. It is assumed that the bearing surfaces are longitudinally rough.

The flow in the medium satisfies the modified form of Darcy's law (Prajapati [23]) while in the film region the equations of hydromagnetic lubrication theory hold. Then, under the usual assumptions of hydromagnetic lubrication the modified Reynolds' equation for the lubricant film pressure (Prajapati [23], Prakash and Vij [1], Vadher et al [24]) is obtained as

$$\frac{1}{x}\frac{d}{dx}\left(x\frac{dp}{dx}\right)=\frac{h\ \dot{\mu}\ A}{\left[\frac{2}{M^3}\left(\tanh\frac{M}{2}-\frac{M}{2}\right)\right]}\cdot\frac{1}{\left[\frac{\phi_0+\phi_1+1}{\phi_0+\phi_1+\frac{\tanh(M/2)}{(M/2)}}\right]} \quad (1)$$

where

$$A = h^{-3}[1-\alpha h^{-1}+6h^{-2}(\sigma^2+\alpha^2)-10h^{-3}(\varepsilon+3\sigma^2\alpha+\alpha^3)]\,(1+4s)/\,(1+2s)$$

Solution of this equation by making use of boundary conditions

$$P\,(a\ \mathrm{cosec}\omega) = 0;\ p\,(b\ \mathrm{cosec}\omega) = 0 \quad (2)$$

determines the distribution of pressure as

$$p = \frac{-\dot{h}\left(a^2-b^2\right)\mathrm{cosec}^2\omega\cdot\left[\frac{\ln(x/b\,\mathrm{cosec}\,\omega)}{\ln(a/b)}-\frac{(x\sin\omega/b)^2-1}{(a/b)^2-1}\right]A}{4\left[\frac{2}{M^3}\left(\tanh\frac{M}{2}-\frac{M}{2}\right)\right]}\cdot\frac{1}{\left[\frac{\phi_0+\phi_1+1}{\phi_0+\phi_1+\frac{\tanh(M/2)}{(M/2)}}\right]}$$

Where $A = h^{-3}[1-\alpha h^{-1}+6h^{-2}(\sigma^2+\alpha^2)-10h^{-3}(\epsilon+3\sigma^2\alpha+\alpha^3)]\cdot(1+4s)/(1+2s)$

The distribution of non - dimensional pressure is obtained

$$P = \frac{-ph^3}{\mu\dot{h}\pi\left(a^2-b^2\right)\mathrm{cosec}\omega}$$

$$=\frac{\mathrm{cosec}\omega\cdot\left[\frac{\ln(x\sin\omega/b)}{\ln(a/b)}-\frac{(x\sin\omega/b)^2-1}{(a/b)^2-1}\right]B}{4\pi\left[\frac{2}{M^3}\left(\tanh\frac{M}{2}-\frac{M}{2}\right)\right]}\cdot\frac{1}{\left[\frac{\phi_0+\phi_1+1}{\phi_0+\phi_1+\frac{\tanh(M/2)}{(M/2)}}\right]} \quad (3)$$

Where in

$$B = \left[1-3\alpha^*+6(\sigma^{*2}+\alpha^{*2})-10(\varepsilon^*+3\sigma^{*2}\alpha^*+\alpha^{*3})\right]\cdot(1+4s^*)/\,(1+2s^*)$$

Where

$$\sigma^* = \frac{\sigma}{h},\qquad \alpha^* = \frac{\alpha}{h},\qquad \varepsilon^* = \frac{\varepsilon}{h^3}$$

Then the load carrying capacity given by

$$w = 2\pi\int_{b\,\mathrm{cosec}\omega}^{a\,\mathrm{cosec}\omega} p\cdot x\,dx$$

is expressed in dimensional form as

$$W = \frac{-\dot{h}\pi\left(a^2-b^2\right)\operatorname{cosec}^4\omega\cdot\left[\left(a^2+b^2\right)-\frac{\left(a^2-b^2\right)}{\ln(a/b)}\right]B}{8\left[\frac{2}{M^3}\left(\tanh\frac{M}{2}-\frac{M}{2}\right)\right]}\cdot\frac{1}{\left[\frac{\phi_0+\phi_1+1}{\phi_0+\phi_1+\frac{\tanh(M/2)}{(M/2)}}\right]}$$

The load carrying capacity is obtained as dimensionless

$$W = -\frac{wh^3}{\mu\dot{h}\pi^2\left(a^2-b^2\right)^2\operatorname{cosec}^2\omega}$$

$$= \frac{\operatorname{cosec}^2\omega\cdot\left[\frac{(a/b)^2+1}{(a/b)^2-1}-\frac{1}{\ln(a/b)}\right]B}{8\pi\left[\frac{2}{M^3}\left(\tanh\frac{M}{2}-\frac{M}{2}\right)\right]}\cdot\frac{1}{\left[\frac{\phi_0+\phi_1+1}{\phi_0+\phi_1+\frac{\tanh(M/2)}{(M/2)}}\right]} \quad (4)$$

Clearly, the distribution of pressure is determined by equation (3), while equation (4) gives the expression for the capacity of load carrying. These performance characteristics are dependent on different parameters such as M, $\phi_0+\phi_1$, σ*,α*, ε*, k, s* and ω. These parameters describe the effect of the cone's magnetization, conductivity, standard deviation, variance, skewedness, aspect ratio and semi - vertical angle, slip parameter respectively. This study reduces observation of Prakash and Vij [1] by setting the roughness parameters, magnetization parameters and conductivity parameters to be zero. Finally, considering the parameters of roughness as zero, this 5study results in the contributions of Shukla and Prasad [26], Dodge et al [26] and Sinha and Gupta [27] in special situations.

III. RESULTS AND DISCUSSIONS:

As the conductivity parameter $\phi_0+\phi_1$ increases, it can be easily noticed that the load carrying capacity increases for fixed values of M, σ*,α*, ε*, k, s* and ω. Moreover, the effect of conductivity on the pressure distribution and load carrying capacity comes through the factor

$$\left(\frac{\phi_0+\phi_1+\frac{\tanh(M/2)}{(M/2)}}{\phi_0+\phi_1+1}\right)$$

This tends to $\frac{\phi_0+\phi_1}{\phi_0+\phi_1+1}$ as tanhM ~ 1, 2 / M ~ 0 for large values of M. It is clear that these two functions increase the functionality $\phi_0 + \phi_1$. From mathematical analysis, It can also be observed that the capacity of carrying pressure and load increases as $\phi_0 + \phi_1$, somewhere else. An interesting point to be noted here is that the bearing with magnetic field can support a load even when there is no flow.

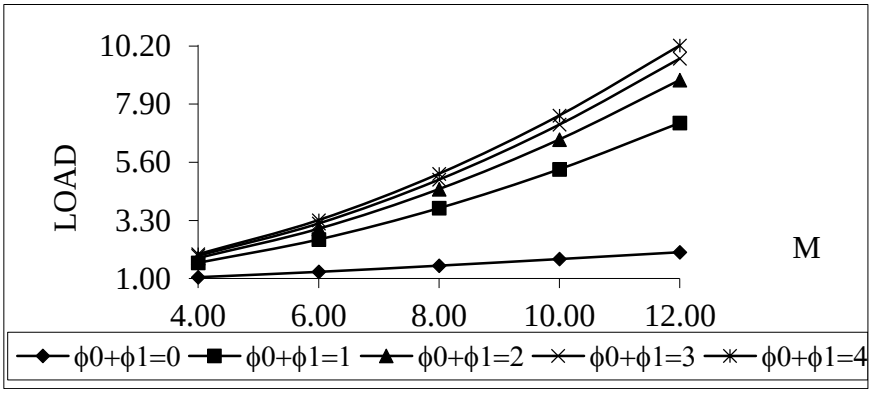

Figure: 1 Variation of load carrying capacity with respect to M and $\phi_0 + \phi_1$

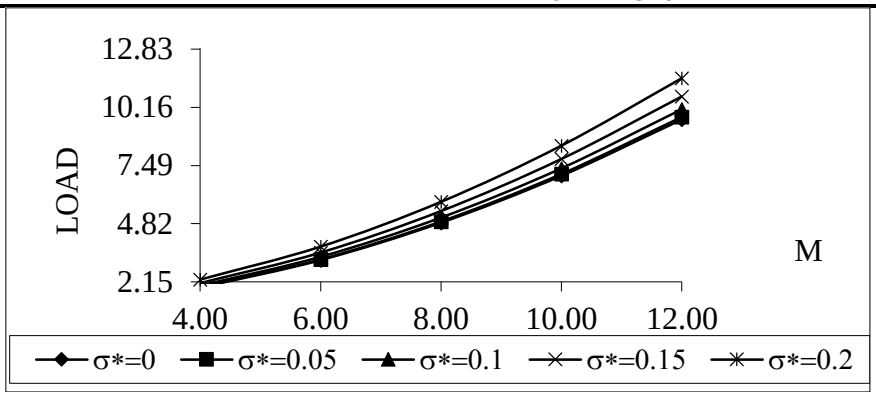

Figure: 2 Distribution of load bearing capacity with respect to M and σ*

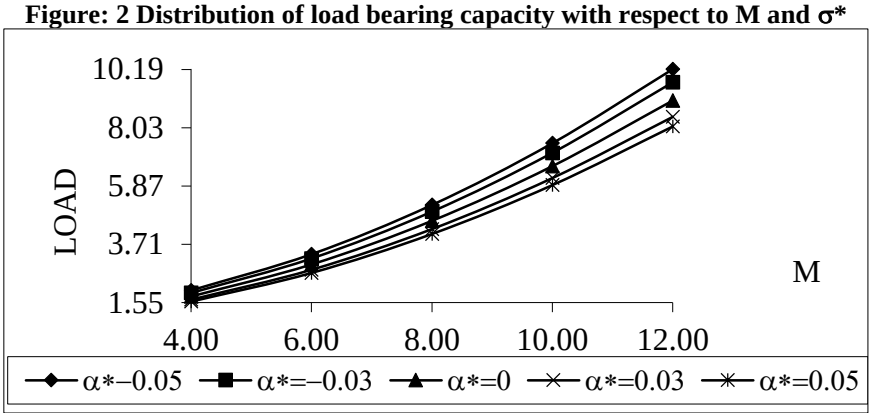

Figure: 3 Profile of load with respect to M and α*

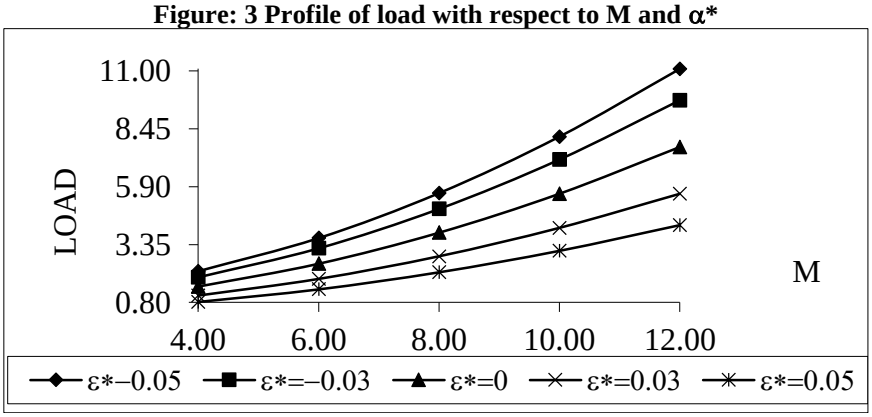

Figure: 4 Variation of load carrying capacity with respect to M and ε*

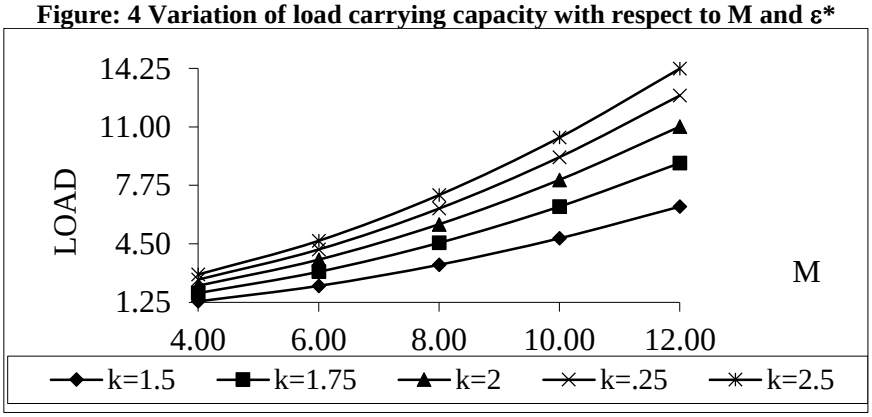

Figure: 5 Distribution of load bearing capacity with respect to M and k

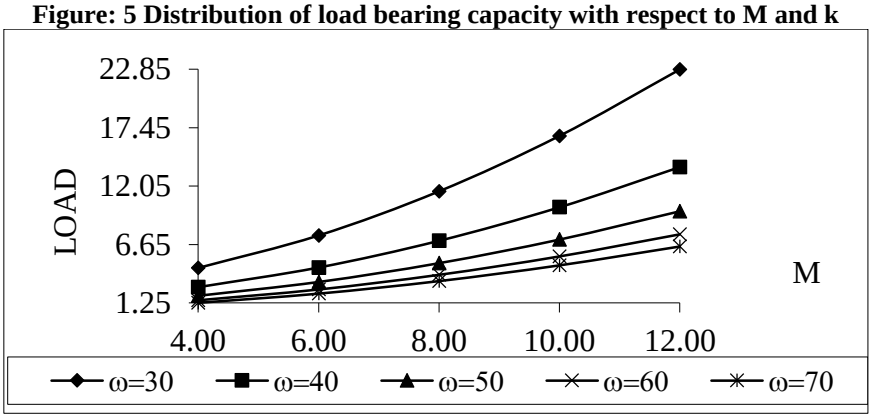

Figure: 6 Distribution of load bearing capacity with respect to M and ω

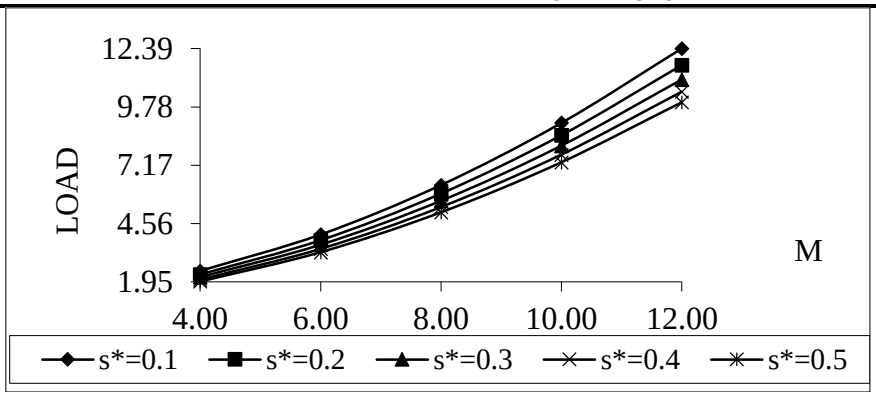

Figure: 7 Distribution of load bearing capacity with respect to M and s*

The variation of the load carrying capacity with respect to the magnetization parameter is shown in Figures (1 - 7) for different values of the conductivity parameter $\phi_0 + \phi_1$,standard deviation σ^* ; variance α^*, skewness ε^*, aspect ratio k, slip parameter s* and semi - vertical angle respectively. From these figures it is clear that the load carrying capacity increases substantially with respect to the parameter of magnetization in which the effect of (-ve) all α^* is the most prevalent, followed by semi-vertical angle ω.

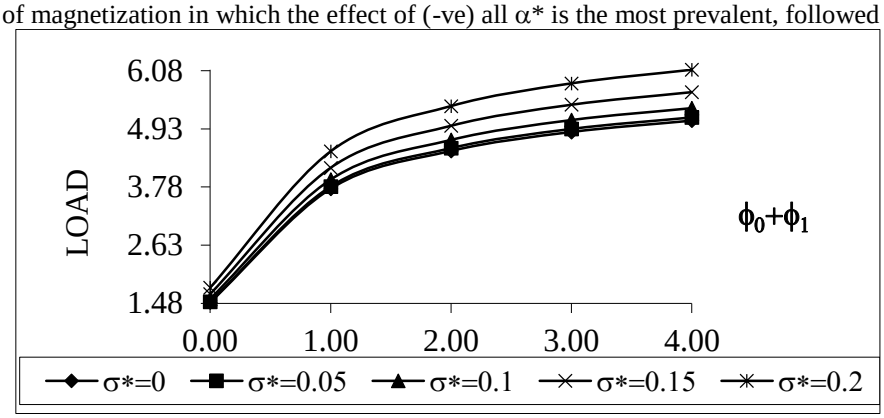

Figure: 8 Profile of load with respect to $\phi_0 + \phi_1$ and σ^*

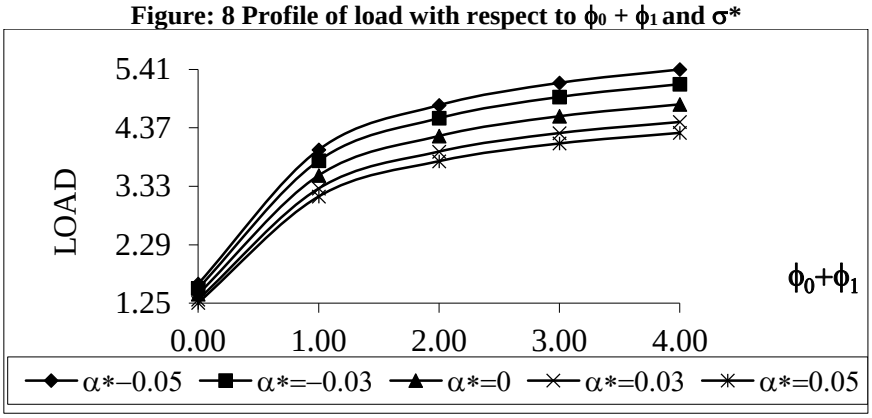

Figure: 9 Variation of load carrying capacity with respect to $\phi_0 + \phi_1$ and α^*

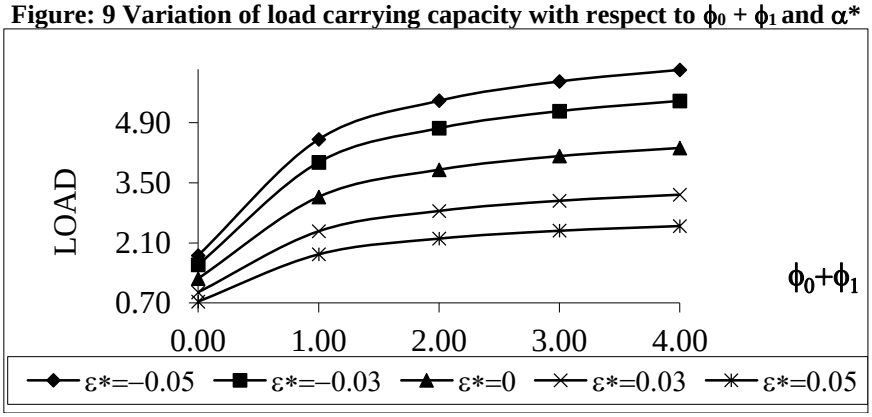

Figure: 10 Distribution of load bearing capacity with respect to $\phi_0 + \phi_1$ and ε^*

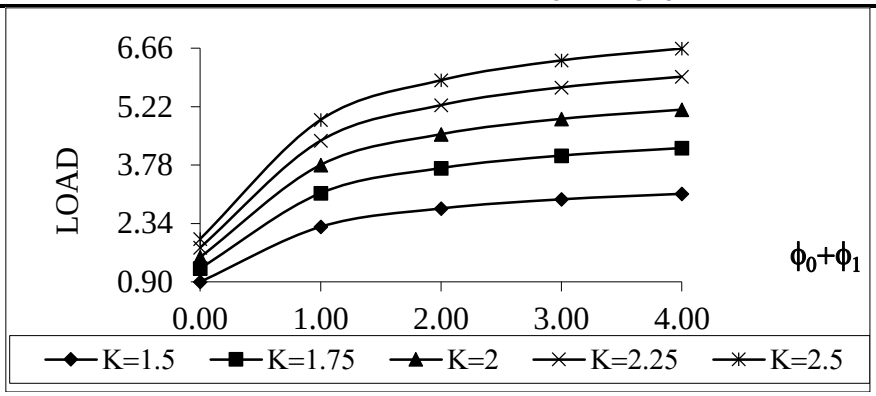

Figure: 11 Profile of load with respect to $\phi_0 + \phi_1$ and k

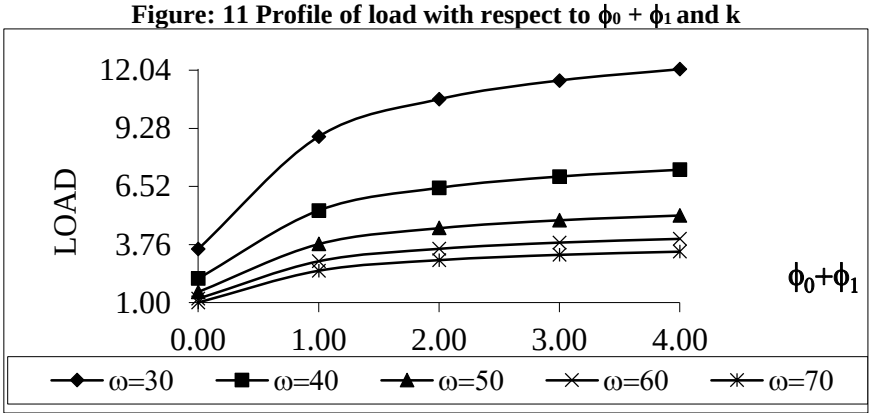

Figure: 12 Profile of load with respect to $\phi_0 + \phi_1$ and ω

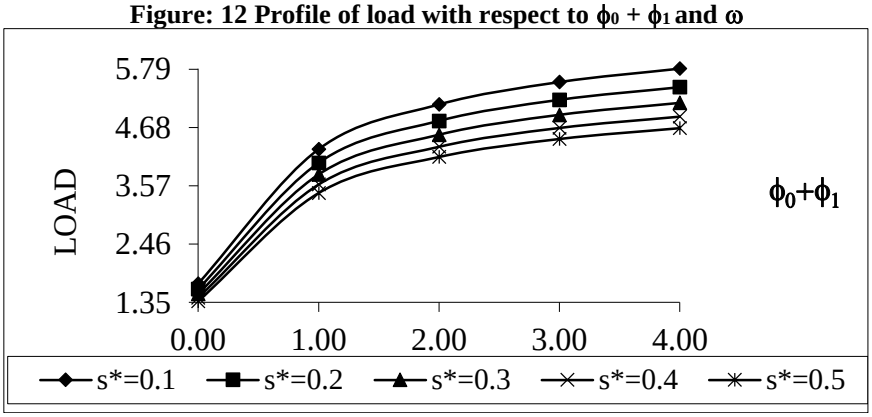

Figure: 13 Profile of load with respect to $\phi_0 + \phi_1$ and s*

Furthermore, the standard deviation initially has a nearly negligible effect and the increase in load arrangement capacity for the combination of M and σ ∗ is relatively less compared to the other cases. In addition, the standard deviation effect is quite negative. Figures (8-13) show the distribution of load carrying capacity with respect to conductivity $\phi_0 + \phi_1$ for multiple parameter values σ*, ε*, α*, k, s* and ω respectively. It is found that the conductivity tends to increase the capacity of the load carrying and the rate of increase in the initial stages is relatively higher. Here, the combined effect of the conductivity and aspect ratio is relatively better than the combined effect of conductivities, while the combined effect of negative ε* and conductivity $\phi_0 + \phi_1$ is comparatively greater than the combined effect of negative α* and conductivity $\phi_0 + \phi_1$. Further, it is noted that the combined effect of conductivity and the aspect ratio lies between the effect of negative variance and skewness so far as the increase in load carrying capacity is concerned.

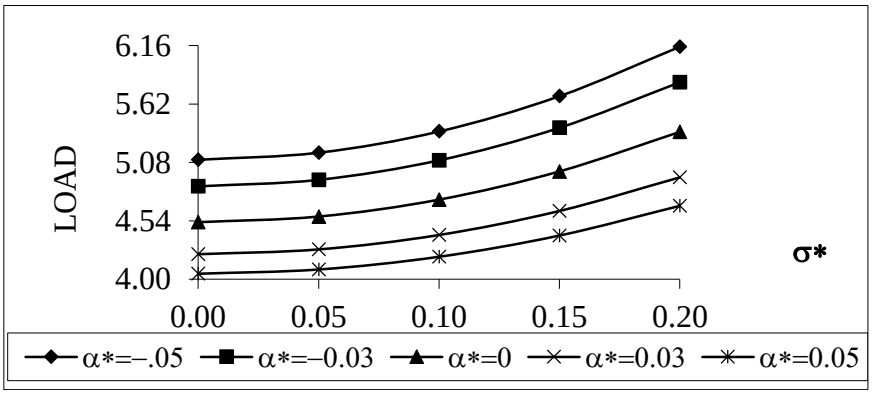

Figure: 14 Variation of load carrying capacity with respect to σ* and α*

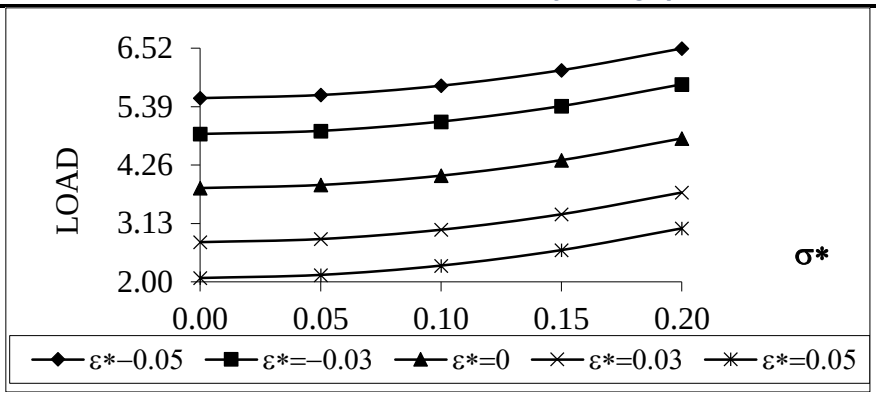

Figure: 15 Distribution of load bearing capacity with respect to σ* and ε*

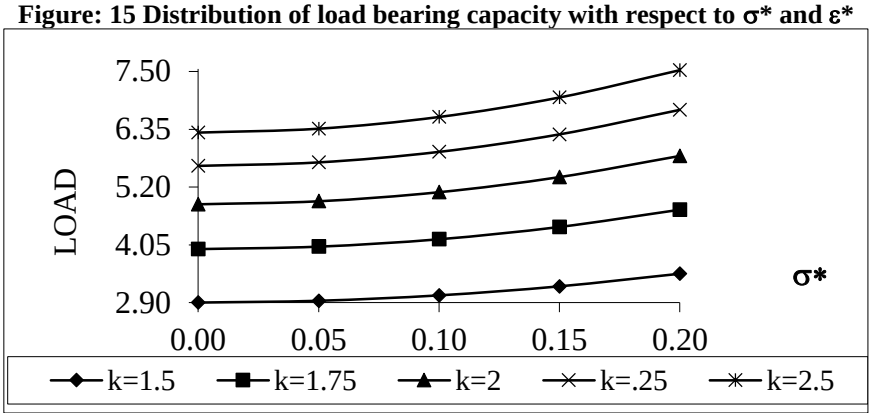

Figure: 16 Profile of load with respect to σ* and k

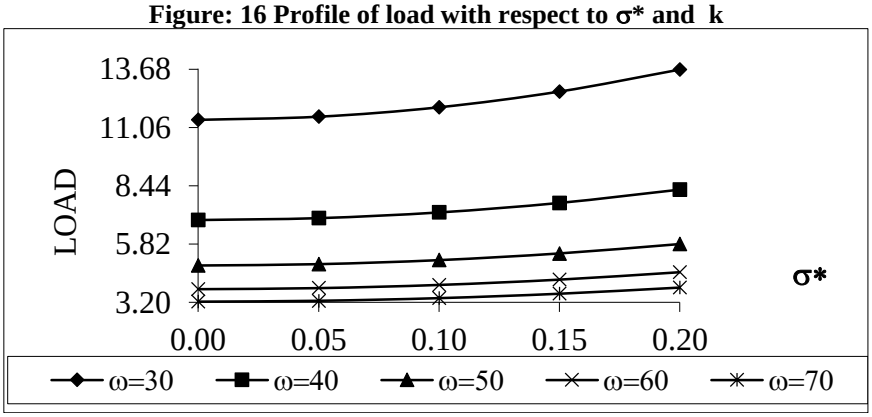

Figure: 17 Profile of load with respect to σ* and ω

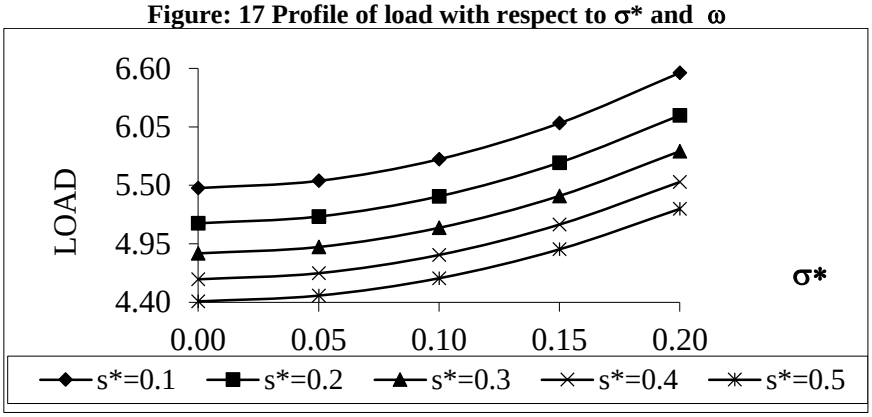

Figure: 18 Profile of load with respect to σ* and s*

Figures (14 - 18) provide the load carrying capacity distribution profile for the standard deviation associated with roughness for different variance, skew, aspect ratio, slip parameter and semi - vertical angle values. The rate of decrease is more pronounced in the case of skewness.

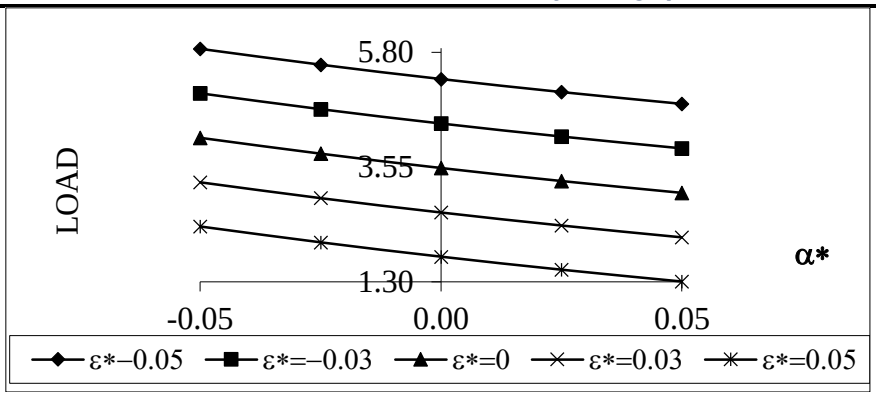

Figure: 19 Variation of load carrying capacity with respect to α* and ε*

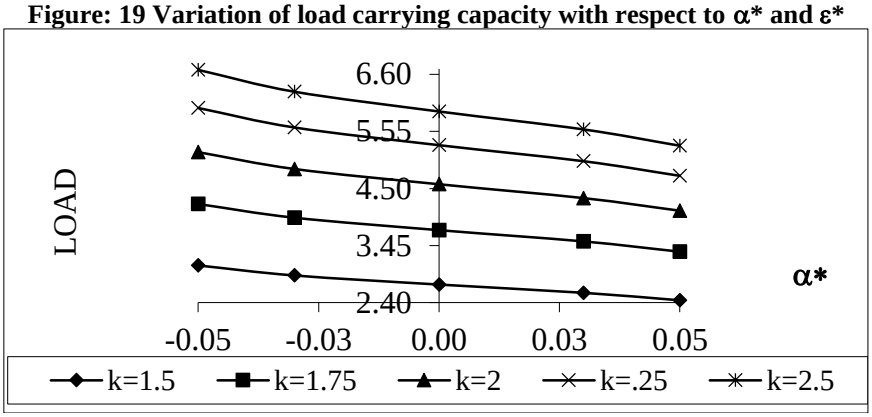

Figure: 20 Distribution of load bearing capacity with respect to α* and k

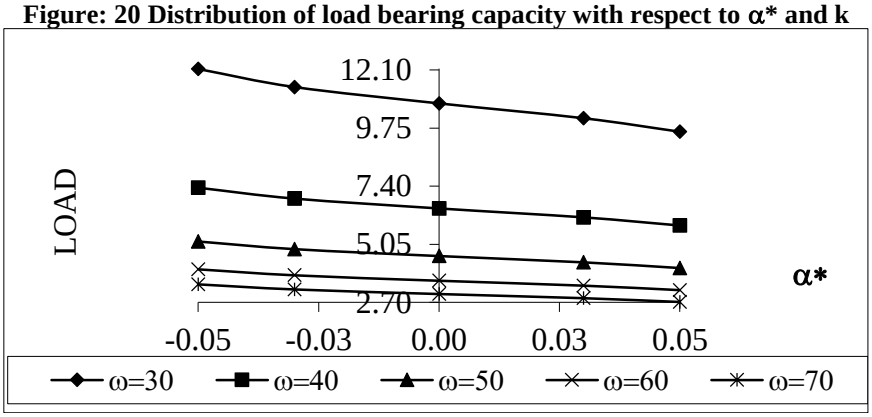

Figure: 21 Distribution of load bearing capacity with respect to α* and ω

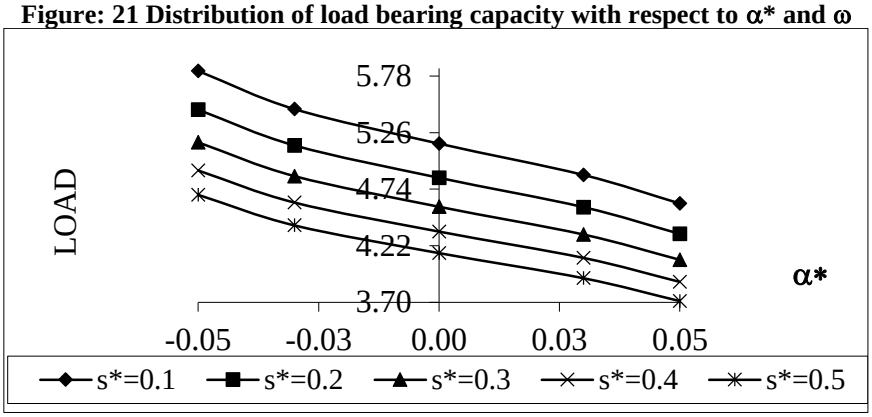

Figure: 22 Distribution of load bearing capacity with respect to α* and s*

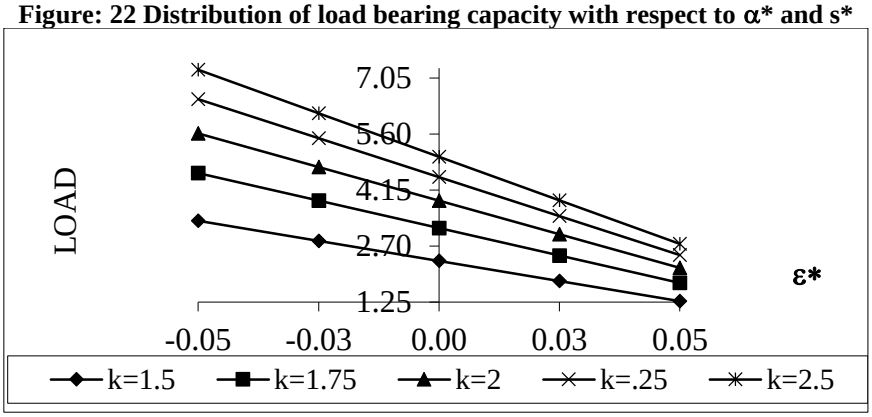

Figure: 23 Profile of load with respect to ε* and k

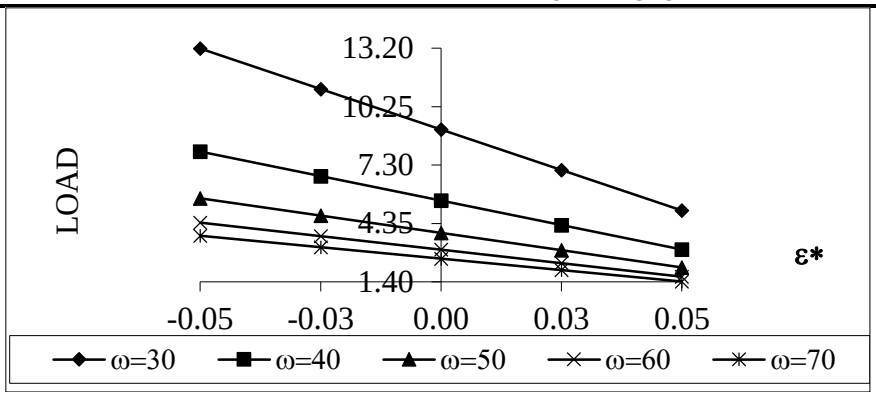

Figure: 24 Profile of load with respect to ε* and ω

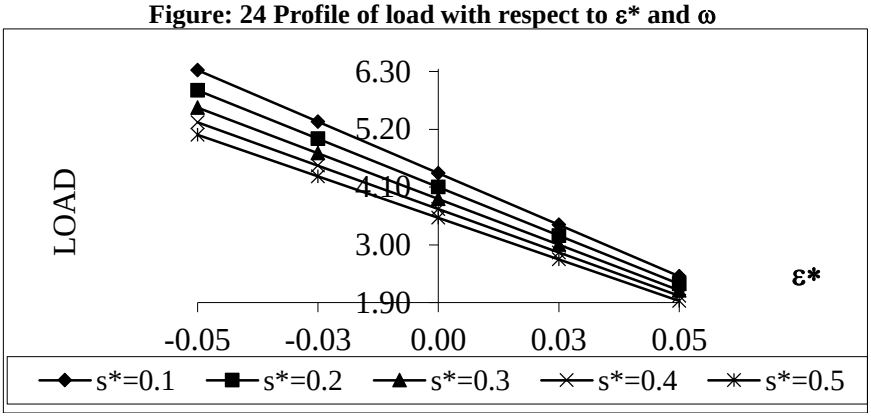

Figure: 25 Profile of load with respect to ε* and s*

Variation of load carrying capacity with respect to the variance for different values of skewness, aspect ratio, slip para meter and the semi vertical angle is presented in Figures (19-22) respectively. While α* (+ve) increases the load carrying capacity, the (-ve) variance increases the load carrying capacity and this rate of increase is more in the case of the aspect ratio. While figures (23-25) shows that the negatively skewed roughness augments the load as in the case of variance (– ve).

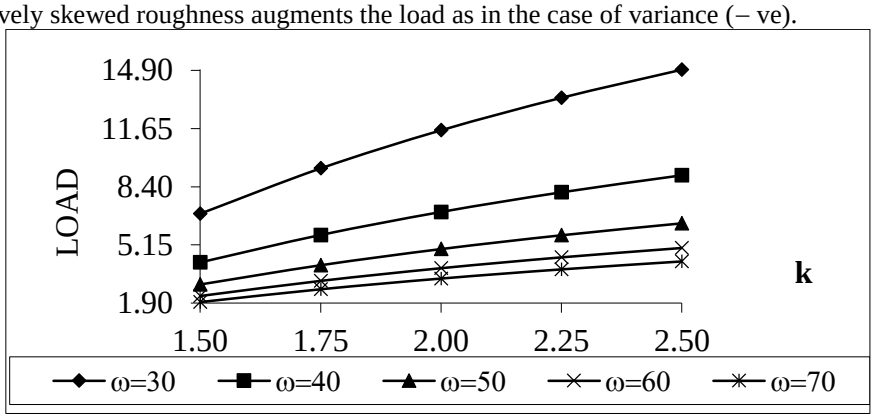

Figure: 26 Profile of load with respect to k and ω

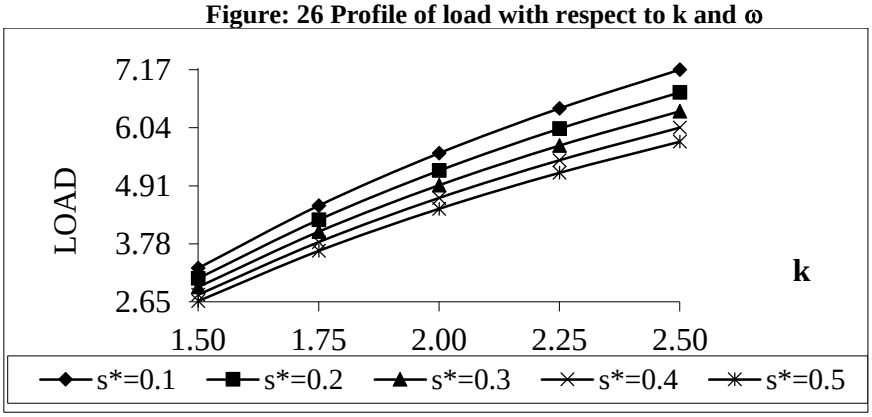

Figure: 27 Profile of load with respect to k and s*

These trends reverse for positively skewed roughness and variance (+ ve).The effect of k and ω is given in Figure (26), which makes it clear that the effect of the aspect ratio is significantly positive, while the load carrying capacity increases with increasing values of the semi-vertical angle. It is appealing to note that this effect on load carrying capacity is increases in the case of aspect ratio k respect to semi-vertical angle ω and slip parameter shows in the Figure (26-27).

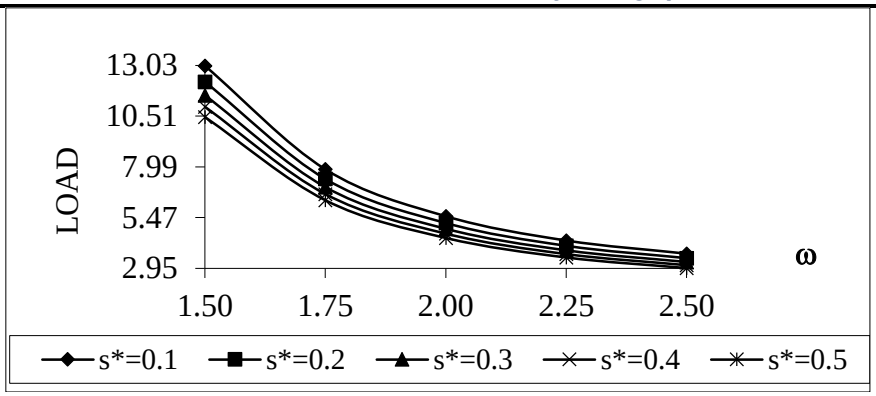

Figure: 28 Profile of load with respect to ω and s*

Further, the effect of slip velocity on the distribution of load carrying capacity increases for higher values of the slip parameter, this can be seen from figure (28).

IV. CONCLUSION:

This analysis strongly recommends that the roughness aspects must be given priority while designing the bearing system. For an overall improved performance of the bearing, the slip parameter is required to be minimized. Further, these types of systems there is a partial effect of hydromagnetization in the case of negatively skewed roughness even when negative variance is involved as load carrying capacity reduces greatly owing to the adverse effect of slip velocity**.**

REFERENCES:

[1] Prakash, J. & Vij, S. K. 1973.Load capacity and time height relation between porous plates. Wear, 24:309-322.
[2] Verma, P. D. S. 1986. Magnetic fluid-based squeeze film. International Journal of Engineering Science, 24(3): 305-401.
[3] Bhat, M. V. & Deheri, G. M. 1991. Squeeze film behavior in porous annular disks lubricated with magnetic fluid. Wear, 151: 123-128.
[4] Bhat, M. V. and Deher, G. M.1992. Magnetic fluid based squeeze film between two curved circular plates. Bulletin of Calcutta Mathematical Society, 85:521-524.
[5] Hsiu. Chiang, Lu. Cheng, Hsu, H. and Lin, J. R. 2004. Lubrication performance of long journal bearings considering effects of couple stresses and surface roughness. Journal of the Chinese Institute of Engineers, 27(2):287-292.
[6] Deher, G. M. Patel, H. and Patel, R. M. 2007. Magnetic fluid-based squeeze film between rough porous truncated conical plates. Journal of Engineering Tribology, 221(J):515-523.
[7] Christensen, H. and Tonder, K. C. 1969a. Tribology of rough surfaces: stochastic models of hydrodynamic lubrication,SINTEF Report No.10/69-18.
[8] Christensen, H. and Tonder, K. C. 1969b. Tribology of rough surfaces: parametric study and comparison of lubrication model, SINTEF Report No.22/69-18.
[9] Christensen, H. and Tonder, K. C. 1970. The hydrodynamic lubrication of rough bearing surfaces of finite width. ASME-ASLE Lubrication Conference.Paper no.70-lub-7.
[10] Gupta, J. L. and Deher, G. 1996. Effect of roughness on the behavior of squeeze film in a spherical bearing. Tribology Transaction, 39:99-102.
[11] Andhariya, P. I. Gupta, J. L. and Deheri, G. 2001. Effects of surface roughness and hydrodynamic lubrications of slider bearings, Tribology Transaction, 44(2):291-297.
[12] Hsu, CH. Lu, R.F. and Lin, J. R. 2009. Combined effects of surface roughness and rotating inertia on the squeeze film characteristics of parallel circular disks. Journal of Marine Science and Technology, 7(1): 60-66.
[13] Schwarz, U. B. 2003. A generalized analytical model for the elastic deformation of an adhesive contact between a sphere and a flat surface. Journal of Colloid and Interface Science, 261(1):99-106.
[14] Shimp, M. E. and Deher, G. 2112a. Magnetic fluid-based squeeze film performance in rotating curved porous circular plates: the effect of deformation and surface roughness. Tribology in Industry, 34(2): 57-67.
[15] Shimp, M. E. and Deher, G. 2012b. A study on the performance of a magnetic fluid-based squeeze film in curved porous rotating rough annular plates and deformation effect. Tribology International, 47: 90-99.
[16] Shimp, M. and Deher, G. 2013. Surface roughness effect on a magnetic fluid-based squeeze film between a curved porous circular plate and a flat circular plate. Journal of the Brazilian Society of Mechanical Sciences and Engineering. (Online).
[17] Shah, R. and Patel, N. 2012. Mathematical modeling of slider bearing of various shapes with combined effects of porosity at both the ends, anisotropic permeability, slip velocity, and squeeze velocity. American Journal of Computational and Applied Mathematics, 2(3):94-100.
[18] Mirea, M. and Voicu, C.O. 2012. Study regarding the bearing capacity of truncated cone and hemispherical foundations realized in punched holes. SGEM2012 Conference Proceedings (June 17-23), 2: 275-282.
[19] Sameh E. Ahmed and Mahdy, A. 2012. Natural convection flow and heat transfer enhancement of a nanofluid Past a truncated cone with magnetic field effect. World Journal of Mechanics, 2(5):272-279.
[20] Nassab, S. A. G. Sohi, H. and Zaim, E. H. 2011. Study of lubricant compressibility effect on hydrodynamic characteristics of heavily loaded journal bearings. Iranian Journal of Science and Technology-Transactions of Mechanical Engineering, 35(M1):101-105.
[21] Rahmatabadi, A. D. And Rashidi, R. 2006. Effect of mount angle on static and dynamic characteristics of gas lubricated, noncircular journal bearings. Iranian Journal of Science and Technology Transaction-B-Engineering, 30(B3):327-337.
[22] Nassab, S. A G. and Moayeri, M. S. 2000. A Two-dimensional thermohydrodynamic analysis of journal bearings characteristics. Iranian Journal of Science and Technology Transaction-B-Engineering, 24(3): 203-220.

[23] Prajapati, B. L. 1995. On certain theoretical studies in hydrodynamic and electromagneto hydrodynamic lubrication. Thesis Sardar Patel University. Vallabh Vidyanagar, Anand, Gujarat, Indi. Ph.D.
[24] Vadhr, P. Deher, G. and Patel, R. M. 2011. Effect of transverse surface roughness on the performance of hydromagnetic squeeze film between conducting truncated conical plate, Journal of marine science And technology, 16(6):673-680.
[25] Shukla, J. B. and Prasad, R. 1965. Hydromagnetic squeeze films between two conducting surfaces. Journal of Basic engineering, Transactions of ASME, 87: 818-822.
[26] Dodge, F. T. Osterle, J. F. and Roulean, WT. 1965. Magnetohydrodynamic squeeze film bearings, Journal of Basic engineering. Transactions of ASME, 87:805-809.
[27] Sinha, P. C. and Gupta, J. L. 1974. Hydromagnetic squeeze films between porous annular disks, Journal of Mathematical and Physical Science, 8:413-422.
[28] Shimp. M. and dehar., G. 2014. Effect of slip velocity and bearing deformation on the performance of a magnetic fluid based rough porous truncated conical plates. IJST Transection of mechanical engineering, 38(M1+):195-206.